Adiabatic Electron Transfer: Comparison of Modified Theory with Experiment

Stephen F. Nelsen *et al.*

Science **278**, 846 (1997);
DOI: 10.1126/science.278.5339.846

Science (print ISSN 0036-8075; online ISSN 1095-9203) is published weekly, except the last week in December, by the American Association for the Advancement of Science, 1200 New York Avenue NW, Washington, DC 20005.

3. J. A. Armstrong *et al.*, *Phys. Rev*. **127**, 1918 (1962); S. Somkeh and A. Yariv, *Opt. Commun*. **6**, 301 (1972).
4. D. Feng *et al.*, *Appl. Phys. Lett*. **37**, 607 (1980); R. L. Byer, *Nonlinear Opt*. **7**, 234 (1994); V. Pruneri, J. Webjorn, J. Russell, D. C. Hanna, *Appl. Phys. Lett*. **65**, 2126 (1995); S. N. Zhu *et al.*, *ibid*. **67**, 320 (1995); H. Ito, C. Takyu, H. Inaba, *Electron. Lett.* **27**, 1221 (1991); M. C. Gupta, W. Kozlovesky, A. C. G. Nutt, *Appl. Phys. Lett*. **64**, 3210 (1994); J. D. Bierlein *et al.*, *ibid*. **56**, 1725 (1990).
5. P. J. Steinhardt and S. Ostlund, *The Physics of Quasicrystals* (World Scientific, Singapore, 1997); C. Janot, *Quasicrystals* (Clarendon Press, Oxford, UK, 1992).
6. S. N. Zhu *et al.*, *Phys. Rev. Lett*. **78**, 2752 (1997); Y. Y. Zhu and N. B. Ming, *Phys. Rev. B* **42**, 3676 (1990); J. Feng, Y. Y. Zhu, N. B. Ming, *ibid.* **41**, 5578 (1990).
7. Y. R. Shen, *The Principles of Nonlinear Optics* (Wiley, New York, 1984).
8. For standard Fibonacci sequence, the ratio is $\tau = (1+\sqrt{5})/2$. The ratios other than τ can be derived from other 1D quasi-periodic subclasses. All possible subclasses have been classified [D. Levine and P. J. Steinhardt, *Phys. Rev. B* **34**, 596 (1986)].
9. The blocks *A* and *B* can also be arranged according to other quasi-periodic subclasses and can be composed of one or more layers of different materials [R. Merlin *et al.*, *Phys. Rev. Lett*. **55**, 1768 (1985); A. Behrooz *et al.*, *ibid*. **57**, 368 (1986)].
10. S. N. Zhu *et al.*, *J. Appl. Phys*. **77**, 5481 (1995).
11. Some essential simplifications of the theoretical treatment were considered, including the approximation of slowly varying envelope for fundamental, second-, and third-harmonic fields and ignoring depletion of the fundamental and harmonic field.
12. By using a special deposition method, B. Hadimioglu *et al.* [*Appl. Phys. Lett*. **50**, 1642 (1987)] fabricated multiple-layer ZnO films with the crystallographic orientation changing for alternating layers.
13. L. A. Gordon *et al.*, *Electron. Lett.* **29**, 1942 (1993).
14. H. W. Mao, F. C. Fu, B. C. Wu, C. T. Chen, *Appl. Phys. Lett.* **61**, 1148 (1992).
15. It was reported that $LiTaO_3$ has short-wavelength transparency from 280 nm [K. Mizuuchi, K. Yamamoto, T. Taniuchi, *ibid*. **58**, 2732 (1991)]. Thus, by a suitable choice of a QPOS, harmonic generation in the UV region is possible.
16. We thank D. Feng for stimulating discussions. Supported by a grant for the Key Research Project in Climbing Program from the National Science and Technology Commission of China.

22 May 1997; accepted 22 September 1997

Adiabatic Electron Transfer: Comparison of Modified Theory with Experiment

Stephen F. Nelsen,* Rustem F. Ismagilov, Dwight A. Trieber II

The radical cations of properly designed bishydrazines allow comparison of observed and calculated electron transfer rate constants. These compounds have rate constants small enough to be measured by dynamic electron spin resonance spectroscopy and show charge transfer bands corresponding to vertical excitation from the energy well for the charge occurring upon one hydrazine unit to that for the electron-transferred species. Analysis of the data for all six compounds studied indicates that the shape of the adiabatic surface on which electron transfer occurs can be obtained from the charge transfer band accurately enough to successfully predict the electron transfer rate constant and that explicit tunneling corrections are not required for these compounds.

Reactions in which a single electron is transferred are extremely important in chemistry and biology and have received a great amount of both experimental and theoretical attention since the seminal theoretical work by Marcus in the late 1950s (*1*, *2*). Marcus introduced a method for estimating the barrier ΔG_{et}^{*} for electron transfer (ET) from three parameters: the vertical reorganization energy λ, the electronic interaction matrix element *V*, and the exothermicity of the reaction $\Delta G°$. In the simplest case (Fig. 1), a $\Delta G° = 0$ reaction, λ is the vertical gap between the minimum on the energy surface of the precursor and the energy surface of the product when neither the solvent nor the internal geometry are allowed to relax. λ is the sum of a solvent contribution (λ_s) and an internal vibrational contribution (λ_v), that is $\lambda = \lambda_s + \lambda_v$. Marcus addressed ways to estimate these quantities (*1*, *2*). The amount of electronic mixing between the precursor and product surfaces is measured by *V*.

In recent years, most experimental and theoretical studies have concentrated on long-distance ET reactions, which are initiated by photoexcitation (*3*). These reactions have small *V* and are usually very exothermic. The most important contributions that have emerged from these studies have been the development of vibronic coupling theory to treat such reactions (*4*) and landmark pulse radiolysis studies (*5*) that established the existence of the "inverted region" predicted by Marcus. Such reactions are involved in the charge separation that occurs in photosynthetic reaction centers (*6*), and the development of fast laser kinetic techniques has been crucial in such studies (*3*, *6*). The great majority of biological ET reactions, however, occur in the dark and have small $\Delta G°$. The present work focuses on a series of carefully designed molecules in which ET occurs with $\Delta G° = 0$ and without photoexcitation. These molecules display optical absorption spectra from which λ and *V* can be estimated, allowing quantitative testing of ET theory.

Symmetrical transition metal–centered intervalence (IV) compounds are conceptually the simplest ET systems and have played a major role in elucidating ET reactions since the first example was prepared in 1969 (*7*). In IV compounds, two metal atoms are connected by a bridging ligand, and the overall charge formally places the metals in different oxidation states. Whether excess charge is delocalized over both metals or localized on one is determined by the relative sizes of λ and *V* (*7*). If $V < \lambda/2$, then charge localization occurs, and there are separate potential energy wells corresponding to the higher charge being on one metal or the other. These wells are displaced from each other on an ET coordinate χ (Fig. 1). If *V* is large enough, a localized IV compound shows a charge transfer (CT) band, which allows measurement of λ.

Hush developed a simple theory for estimating both λ and *V* from such IV-CT bands (*8*). Marcus (*1*, *2*) and Hush (*8*) assume that the diabatic energy surfaces (the energy wells in the absence of electronic coupling) are parabolas in a plot of energy versus χ. In this case, the transition energy at the IV-CT maximum (E_{op}) is equal to λ. Hush's estimate of *V* (cm^{-1}), which we shall designate as V_H to distinguish it from other estimates, is

$$V_H = (0.0206/d)(\Delta\nu_{1/2}\varepsilon_{max}E_{op})^{1/2} \quad (1)$$

where *d* (Å) is the ET distance, $\Delta\nu_{1/2}$ (cm^{-1}) is the IV-CT band width at half-height, and ε_{max} ($M^{-1}cm^{-1}$) is the molar extinction coefficient at the band maximum. Tunneling corrections are also assumed to be necessary to calculate the ET rate constant k_{et} (*1*, *2*, *8*). Estimation of the size of the tunneling correction requires knowing the averaged energy $h\nu_v$ (where *h* is Planck's constant) of the vibrational frequencies ν_v active in the ET process, which Hush also estimated from the IV-CT band width (*8*).

Symmetrical IV compounds would provide the most direct test of the validity of the ET parameters derived from their IV-CT bands, allowing comparison of the calculated rate constant with the experimental value. Unfortunately no adequate method exists for measuring the large values of k_{et} predicted for transition metal IV compounds (*3*). There is no transient to follow

Department of Chemistry, University of Wisconsin, Madison, WI 53706–1396, USA.

*To whom correspondence should be addressed. E-mail: nelsen@chem.wisc.edu

for ET within symmetrical IV compounds, precluding the use of fast laser kinetic measurements (*9*–*11*). We have prepared organic analogs of IV compounds that solve the problem of measuring k_{et} and report a classical analysis of IV-CT bands that focuses on proper estimation of the adiabatic energy surface on which ET occurs. Parameters derived from the IV-CT bands allow accurate estimation of k_{et} for our compounds without the need for explicit tunneling corrections.

We have developed IV compounds containing hydrazines as the charge-bearing units. These IV compounds have much smaller values of k_{et} than the transition metal–centered compounds, even when V is rather large, because hydrazines have far larger values of λ_v than metal complexes. We can adjust k_{et} for our compounds such that it becomes measurable by dynamic electron spin resonance (ESR), because λ_v and V are adjustable by changes in the substituents at the nitrogens and λ_s is sensitive to solvent. For the nitrogen splitting constant of ~13 G for a hydrazine radical cation, the ESR spectrum is sensitive to intramolecular ET in an IV compound when k_{et} is near 10^8 s^{-1} (*12*). We found that bishydrazines linked by two sets of four σ bonds have high enough ε_{max} for convenient study by optical spectroscopy (*12*). Alteration of the remaining substituents produced compounds that were sufficiently stable in the IV oxidation state (+1) and had values of k_{et} large enough to measure (Fig. 2). The completely N,N′-bicyclic-substituted compound $\mathbf{1}^+$ has k_{et} near 10^8 at room temperature in acetonitrile (AN) (*13*). Compounds with unlinked third alkyl substituents at nitrogen ($\mathbf{2}^+$ to $\mathbf{4}^+$) have higher λ_v, and k_{et} is too small to measure accurately without thermal decomposition in AN, but we were able to measure k_{et} near room temperature using a solvent with lower λ_s, methylene chloride (MC) (*14*). Attaching diazabicyclooctyl groups in para positions on a benzene ring provided an aromatic-bridged compound, but k_{et} was too large to be measured accurately (*15*). Substitution of methyls for the ring hydrogens ($\mathbf{5}^+$ and $\mathbf{6}^+$) increased the N-aryl twist angle, decreasing V and k_{et}. Both $\mathbf{5}^+$ and $\mathbf{6}^+$ have measurable k_{et} in the temperature range $T = 245 \pm 10$ K in AN and 200 ± 15 K in MC (*16*). These studies have provided eight sets of experimental $k_{et}(T)$ data for comparison with rate constants calculated from optically derived ET parameters.

Marcus-Hush theory assumes parabolic diabatic energy surfaces (Fig. 1). Electronic coupling V produces the double-well adiabatic energy ground-state surface E_1 and excited-state surface E_2. There is an avoided crossing ($E_2 - E_1 = 2V$) at $X = 0.5$ (*1*, *2*, *8*). This is true for large values of V as well as the small values for which the expressions were originally derived (*17*). Using parabolic diabatic surfaces, the IV-CT band width depends only on E_{op}; the band width at half height is Hush's high-temperature limit (htl) value, $\Delta\nu_{1/2}^{htl} = [16RT(\ln 2)E_{op}]^{1/2}$, where R is the gas constant, and the band is symmetrical about E_{op}. Experimental IV-CT bands are significantly broader than $\Delta\nu_{1/2}^{htl}$ and are broader on the high-energy side of E_{op} than on the low-energy side (*4*, *7*, *9*). For our compounds, $\Delta\nu_{1/2}^{obs}/\Delta\nu_{1/2}^{htl}$ ranged from 1.15 to 1.68. Hush rationalized observed band widths larger than $\Delta\nu_{1/2}^{htl}$ by introducing dependence of band width on $h\nu_v$. He used tunneling factors depending on the contribution of each component of $h\nu_v$ to ν_v in calculating k_{et} (*8*). Application of his equations to our compounds produces calculated rate constants that are too small if tunneling is ignored. Hush's tunneling equations are only supposed to be valid when $h\nu_v < 2RT$, and most of the active modes estimated by dynamics calculations on $\mathbf{1}^+$ are larger (*18*). Not surprisingly, use of Hush's tunneling equations outside the range in which they are valid does not give the experimental rate constants; the calculated ones are too large.

The IV-CT absorption bands that have the observed shape (*14*, *16*) can be simulated well by the equations derived from vibronic coupling theory (*19*). Band simulation is important because experimental data typically have at least some overlap of the IV-CT band with the tails of other bands, and if band shape simulation cannot be used, there is no good criterion for assessing band width accurately. Although ET parameters giving good fit to the IV-CT bands were obtained, there are serious problems in applying vibronic coupling theory to rate constant calculations for our compounds. The separation of λ into λ_v and λ_s is critical for calculation of k_{et}, but separation based on the band simulations proved ambiguous because the calculated λ_v/λ_s is sensitive to $h\nu_v$, and consistent values of λ_s and λ_v were not obtained when the same compound was examined in different solvents (*14*, *16*). The vibronic coupling constant ($S = \lambda_v/h\nu_v$) is large for our compounds, requiring the potential-energy surface to remain harmonic to past the 14th vibrational level (which seems unlikely) for vibronic coupling theory to work quantitatively. The IV-CT band analysis is sensitive to the vibrational level separations near vibrational levels *S*, but the rate constant calculation is only sensitive to separations of vibrational levels 0 to 4. When k_{et} was calculated using Jortner's double-sum rate equation, values too small by factors of >20 were obtained (*14*, *16*).

The rather large values of V for our compounds place their intramolecular ET firmly in the adiabatic rate regime (*1*, *2*). Adiabatic reactions are those in which a system crosses from one energy well to another with a probability (κ_{el}) of unity when sufficient thermal energy is available; $\kappa_{el} > 0.99$ for $\mathbf{1}^+$ through $\mathbf{6}^+$ (*20*). As V becomes small, κ_{el} becomes much less than 1, and a reaction becomes significantly nonadiabatic. In nonadiabatic reactions, k_{et} is principally determined by vibronic coupling (*1*–*4*).

We use the "semiclassical" adiabatic rate equation (*2*)

$$k_{et,ad} = \nu_v(\lambda_v/\lambda)^{1/2}\exp(-\Delta G^*/RT) \quad (2)$$

where the ET rate constant is only linearly dependent on $h\nu_v$ and is quite insensitive to the partitioning between λ_s and λ_v. The

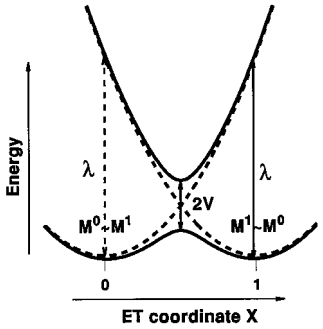

Fig. 1. Marcus-Hush diagram for ET within a +1 charged symmetrical IV compound. The simplest case, $\Delta G° = 0$, is shown. The parabolic diabatic energy surfaces are shown as broken lines, and the adiabatic surfaces for electronic coupling V (drawn for $V = \lambda/8$) are shown as solid lines. Vertical energy gaps at the energy minima for both the diabatic parabolic surfaces (shown in the left well) and the adiabatic surfaces (shown in the right well) are $\lambda = E_{op}$.

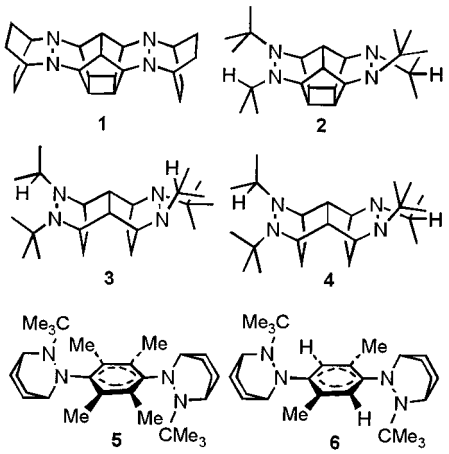

Fig. 2. Structures of the bishydrazines giving radical cations for which k_{et} has been measured. Me, methyl (CH_3).

only critical parameter is ΔG^*, the energy difference between E_1 at the ET transition-state maximum and at the energy minimum for the system (*21*, *22*). The problem of estimating k_{et} for our adiabatic reactions is thus essentially reduced to finding a sufficiently accurate representation of E_1 as a function of χ to allow extrapolation from χ_{min} to $\chi = 0.5$. We therefore have turned our attention to determining E_1 as a function of χ from the IV-CT band. Optical absorption band shape determined from classical theory maps the ground- and excited-state adiabatic energy surfaces through the Boltzmann factor $\varepsilon_{rel} = \varepsilon/\varepsilon_{max} = \exp[-(E_1 - E_{1,min})/RT]$ and the photon energy $h\nu = E_2 - E_1$. Thus, at 298 K, ε_{rel} drops to 0.5 when E_1 is 144 cm^{-1} higher than the minimum, and the vertical energy gaps between E_1 and E_2 at these points on the E_1 surface are given by the $h\nu$ values (Fig. 3). This allows calculation of IV-CT band shape from adiabatic surfaces without knowledge of the vibronic coupling parameters that produced these surfaces. These parameters are, in principle, very complex (*22*). An IV compound thus reveals its adiabatic ET surfaces near χ_{min} through its IV-CT band, and adiabatic surfaces that fit a symmetrical IV-CT band must have the correct relative shapes for χ about −0.2 to +0.2 (on the ground-state surface) and +0.8 to +1.2 (on the excited-state surface).

The adiabatic surfaces used in Marcus-Hush theory are derived by solving a two-state secular determinant with quadratic diabatic Hamiltonian matrix elements $H_{aa} = \lambda\chi^2$ and $H_{bb} = \lambda(1 - \chi)^2$ (*1*, *2*, *17*). To obtain adiabatic energy surfaces that fit the CT bands, we solved the secular determinant using modified "quartic augmented" matrix elements having a $C\chi^4$ quartic term and a $1/(1 + C)$ normalization term

$$H'_{aa} = [\lambda\chi^2/(1 + C)][1 + C\chi^2]$$
$$H'_{bb} = [\lambda(1-\chi)^2/(1+C)][1+C(1-\chi)^2] \quad (3)$$

When $C = 0$, Eq. 3 gives the Marcus-Hush quadratic matrix elements. The width of the CT bands calculated using the modified diabatic surfaces can be adjusted by changing C. For our compounds, fits to the experimental spectra were obtained with $C = 0.1$ to 0.3. The principal effect of increasing C is to make the diabatic curves cross at a smaller energy value than the value of $\lambda/4$ for $C = 0$ parabolas. Crossing occurs at an energy that is smaller by the fraction $(1 + C/4)/(1 + C)$ (for example, 0.875 at $C = 0.2$). This change makes the ET barrier calculated for the adiabatic surfaces, $\Delta G^* = E_{1,max} - E_{1,min}$, substantially smaller than that for $C = 0$ parabolas (*23*). The minima on the ground-state adiabatic surface move positive of $\chi = 0$ and negative of 1 as V increases, and the observed width in χ increases as C increases, making the interpolation to $\chi = 0.5$ smaller.

The experimental and calculated rate constants are compared in Table 1. We designate the experimental k_{et} interpolated or extrapolated to 300 K from the ESR data as k_{esr}, and the $k_{et,ad}$ calculated from Eq. 2 using the parameters that give best fit to the optical band at room temperature as k_{opt}. For all six compounds, we used $h\nu_v = 800$ cm^{-1}, close to the value estimated by dynamics calculations on $\mathbf{1}^+$ (*18*). The value of $k_{et,ad}$ is rather insensitive to λ_s and λ_v. We partitioned λ_v and λ_s on the basis of Marcus's dielectric continuum λ_s equation (*1*, *2*), which can be written as (λ in kcal/mol) $\lambda_s(AN) = 3.64[\lambda(AN) - \lambda(MC)]$, assuming λ_v to be the same in both solvents (*14*). This partitioning puts $(\lambda_v/\lambda)^{1/2}$ in the narrow range 0.75 to 0.89 for our compounds (*24*). There is currently uncertainty about evaluating V from IV-CT bands. Young and co-workers introduced a dependence on the refractive index *n* of the solvent in calculation of V when they derived vibronic coupling theory fits to IV-CT bands (*19*). Dependence of V on *n* does not appear in Hush's equation (Eq. 1) (*8*). It is not clear which formulation is to be preferred, and we therefore consider both Hush's traditional V_H and the lower value $V_L = V_H/(n)^{1/2}$, which is the expression of (*19*) applied to classical theory (*25*, *26*). In almost every instance, the V_L values produce a k_{opt}/k_{esr} ratio closer to unity than do the V_H values (Table 1). The k_{opt}/k_{esr} ratios using V_L are close to 1 (range: 0.9 to 1.6) for the σ-bridged examples, where 300 K is within the temperature range studied. As might be anticipated, agreement is not as good for the aromatic-bridged examples, where k_{esr} had to be extrapolated from measurements at 245 ± 10 K in AN and 200 ± 15 K in MC. The largest ratio (for $\mathbf{6}^+$ in MC) is under 4, and even this calculation is probably still within experimental error of k_{esr}.

The observed IV-CT band shape demonstrates that parabolic diabatic energy surfaces should not be used in a Marcus-Hush double potential-well analysis intended to produce adiabatic surfaces. Simple classical CT band analysis, using quartic-augmented diabatic surfaces that actually fit the IV-CT band, appears to allow accurate estimation of the classical ET barrier (ΔG^*), because the calculated rate constant produces excellent agreement

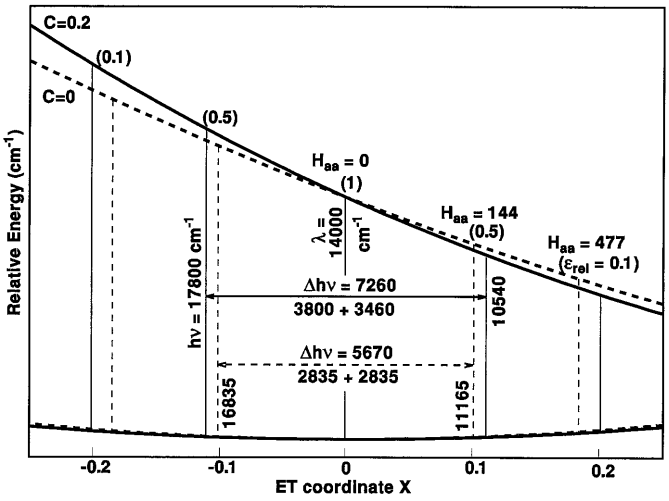

Fig. 3. Origin of the larger band width and asymmetry for quartic-augmented diabatic surfaces. The hypothetical $V = 0$ case is illustrated for simplicity. Parabolic $C = 0$ (broken lines) and $C = 0.2$ (solid lines) diabatic energy surfaces near the energy minimum at $X = 0$, drawn for $\lambda = 14{,}000$ cm^{-1} at 25°C are shown, with the vertical energy gaps $h\nu$ corresponding to $\varepsilon_{rel} = 0.5$ for both surfaces, as well as positions on the X coordinate for the $\varepsilon_{rel} = 0.1$ gaps.

Table 1. Comparison of observed and calculated ET rate constants.

Compound	Solvent	k_{ESR} (10^8 s^{-1})	V_L (kcal/mol)	V_H (kcal/mol)	k_{opt}/k_{ESR} Using V_L	k_{opt}/k_{ESR} Using V_H
$\mathbf{1}^+$	AN	1.3	3.37	3.76	1.1	2.0
$\mathbf{2}^+$	MC	1.3	2.52	3.00	1.6	3.3
$\mathbf{3}^+$	MC	1.1	3.02	3.60	0.9	2.0
$\mathbf{4}^+$	MC	1.0	3.02	3.60	0.9	2.0
$\mathbf{5}^+$	AN	8.6	2.84	3.29	0.6	1.2
$\mathbf{5}^+$	MC	37.6	2.77	3.31	1.1	2.2
$\mathbf{6}^+$	AN	5.4	4.22	4.88	1.6	3.4
$\mathbf{6}^+$	MC	24.5	4.10	4.90	3.6	8.8

with experiment. This agreement suggests that our procedure accurately evaluates λ and V for these systems. It is noteworthy that, for the strongly adiabatic systems studied here, classical theory that ignores tunneling reproduces the observed rate constant, even though $h\nu_v$ modes far larger than $2RT$ are involved. We suggest that this success means that tunneling effects have been effectively incorporated into the calculated ground-state adiabatic surface by our band-fitting procedure. To our knowledge, there have been no prior comparisons of calculated rate constants based on optically determined ET parameters with experimental ones for ET processes that occur in the adiabatic rate regime. Our results verify that Hush's method for extracting V is quantitatively correct in the absence of intensity borrowing problems (*10*). The dependence on the solvent's refractive index introduced by Young and co-workers apparently produces a more accurate V value. For our high-S and high-V cases, classical theory is more accurate for estimating rate constants than is the use of vibronic coupling theory outside the parameter ranges for which it was designed (*27*). It remains to be seen how well a similar approach using κ_{el} in Eq. 2 will work when V is smaller and the ET reaction is not strongly adiabatic.

REFERENCES AND NOTES

1. R. A. Marcus and N. Sutin, *Biochim. Biophys. Acta* **811**, 265 (1985).
2. N. Sutin, *Prog. Inorg. Chem.* **30**, 441 (1983).
3. P. F. Barbara, T. J. Meyer, M. A. Ratner, *J. Phys. Chem.* **100**, 13148 (1996).
4. J. Jortner and J. Ulstrup, *J. Chem. Phys.* **63**, 4358 (1975); J. Jortner and M. Bixon, *ibid.* **88**, 167 (1988); J. Cortes, H. Heitele, J. Jortner, *J. Phys. Chem.* **98**, 2527 (1994).
5. G. L. Closs and J. R. Miller, *Science* **240**, 440 (1988).
6. M. R. Wasielewski, *Chem. Rev.* **92**, 435 (1992).
7. C. Creutz, *Prog. Inorg. Chem.* **30**, 1 (1983); K. Prassides, Ed., *Mixed Valency Systems: Applications in Chemistry, Physics, and Biology* (NATO ASI Ser., Kluwer Academic, Dordrecht, Netherlands, 1991).
8. N. S. Hush, *Prog. Inorg. Chem.* **8**, 391 (1967); *Coord. Chem. Rev.* **64**, 135 (1985).
9. There are significant problems in determining values of V for ET within photoexcited asymmetrical systems, which do have a transient to follow. Electronic mixing of the IV state with locally excited states is allowed, and both CT band intensities and back-ET rate constants are greatly affected by them. Good agreement with theory is obtained, but neither k_{et} nor ε_{max} relates to the V shown in Fig. 1 (*10*). For example, the V values estimated for Paddon-Row's σ-bridged aromatic, cyanoolefin systems (*11*), which appeared to be the best-documented series of such measurements available, have recently been retracted, with the statement that both the CT band intensities and back-ET rate constants are basically determined by mixing of the IV state with locally excited states (*10*).
10. M. Bixon, J. Jortner, J. W. Verhoeven, *J. Am. Chem. Soc.* **116**, 7349 (1994).
11. N. S. Hush *et al.*, *Chem. Phys. Lett.* **117**, 8 (1985); H. Oevering *et al.*, *J. Am. Chem. Soc.* **109**, 3258 (1987); M. N. Paddon-Row *et al.*, *J. Phys. Chem.* **92**, 6958 (1988); H. Oevering, J. W. Verhoeven, M. N. Paddon-Row, J. M. Warman, *Tetrahedron* **45**, 4751 (1989); J. M. Warman *et al.*, *J. Phys. Chem.* **95**, 1979 (1991); J. Kroon, J. W. Verhoeven, M. N. Paddon-Row, A. M. Oliver, *Angew. Chem. Int. Ed. Engl.* **30**, 1358 (1991); J. Kroon *et al.*, *J. Phys. Chem.* **97**, 5065 (1993).
12. S. F. Nelsen, H. Chang, J. J. Wolff, J. Adamus, *J. Am. Chem. Soc.* **115**, 12276 (1993).
13. S. F. Nelsen, J. Adamus, J. J. Wolff, *ibid.* **116**, 1589 (1994).
14. S. F. Nelsen, M. T. Ramm, J. J. Wolff, D. R. Powell, *ibid.* **119**, 6863 (1997).
15. S. F. Nelsen, R. F. Ismagilov, D. R. Powell, *ibid.* **118**, 6313 (1996).
16. ———, *ibid.*, in press.
17. C. Creutz, M. D. Newton, N. Sutin, *J. Photochem. Photobiol. A* **82**, 47 (1994).
18. S. F. Nelsen, *J. Am. Chem. Soc.* **118**, 2047 (1996).
19. I. R. Gould *et al.*, *Chem. Phys.* **176**, 439 (1993).
20. We obtained κ_{el} using equations 36 through 38 in (*2*), with the $h\nu_v = 800\ cm^{-1}$ used here.
21. Knowledge of ΔG^* is far from sufficient to calculate k_{et} for a nonadiabatic case, where k_{et} is controlled by Franck-Condon factors, which in principle require a detailed knowledge of the contribution of all of the many modes (*22*) making up λ_v for their calculation. The adiabatic nature of our systems makes calculation of k_{et} far simpler than the case for nonadiabatic ET systems.
22. S. K. Doorn and J. T. Hupp, *J. Am. Chem. Soc.* **111**, 1142 (1989); A. B. Meyers, *Chem. Rev.* **96**, 911 (1996).
23. The quartic-augmented surfaces produce a value of λ that is slightly higher than E_{op} but closer to E_{op} than the λ obtained using vibronic coupling theory fits to the same data. $E_{1,min}$ is slightly more negative than $-V^2/\lambda$ obtained using parabolas, but the effect on $E_{1,max}$ is much larger. Use of $\Delta G^* \cong (\lambda/4)(1 + C/4)/(1 + C) - V + V^2/\lambda$ provides an excellent approximation to ΔG^* for our compounds.
24. We have evidence that the dielectric continuum approximation is a rather poor assumption for all of these compounds except for $\mathbf{1}^+$, and that it overestimates λ_s. Use of a smaller λ_s would make $(\lambda_v/\lambda)^{1/2}$ even closer to 1 and would not affect the estimation of $k_{et,ad}$ significantly.
25. The $n^{-1/2}$ dependence for V described in (*19*) arises from the use of a refractive index factor $f(n) = n^3$ in an expression for radiative emission (their equation 3). More recently, these authors have suggested using a more complex expression, $f(n) = n[(n^2 + 2)/3]^2$ [equation 3b of (*26*)], which they note produces a contribution that is about 11% smaller with a virtually identical dependence on n; they also indicate in appendix 3 (*26*) that the true dependence may be even more complicated.
26. I. R. Gould, R. H. Young, L. J. Mueller, A. C. Albricht, S. Farid, *J. Am. Chem. Soc.* **116**, 8188 (1994).
27. Because use of only λ and C fits the experimental IV-CT band shape, it is hardly surprising that, when the same data are fit using the three parameters of vibronic coupling theory (λ_s, λ_v, and $h\nu_v$), strong interaction of these parameters results (*14*, *16*). In studies using vibronic coupling theory to fit optical band shape or plots of k_{et} and $\Delta G°$, it is usually stated that all three parameters were determined from the fit. This determination cannot be made for any of our data because of the strong interaction of these parameters.

28. We thank the National Science Foundation for partial financial support of this work through grant CHE-9417946 and R. Young, for extended discussions.

16 July 1997; accepted 22 September

Structure of the Carboxyl-Terminal Dimerization Domain of the HIV-1 Capsid Protein

Theresa R. Gamble,* Sanghee Yoo,* Felix F. Vajdos, Uta K. von Schwedler, David K. Worthylake, Hui Wang, John P. McCutcheon, Wesley I. Sundquist,† Christopher P. Hill†

The carboxyl-terminal domain, residues 146 to 231, of the human immunodeficiency virus–1 (HIV-1) capsid protein [CA(146–231)] is required for capsid dimerization and viral assembly. This domain contains a stretch of 20 residues, called the major homology region (MHR), which is conserved across retroviruses and is essential for viral assembly, maturation, and infectivity. The crystal structures of CA(146–231) and CA(151–231) reveal that the globular domain is composed of four helices and an extended amino-terminal strand. CA(146–231) dimerizes through parallel packing of helix 2 across a dyad. The MHR is distinct from the dimer interface and instead forms an intricate hydrogen-bonding network that interconnects strand 1 and helices 1 and 2. Alignment of the CA(146–231) dimer with the crystal structure of the capsid amino-terminal domain provides a model for the intact protein and extends models for assembly of the central conical core of HIV-1.

The 26-kD capsid protein (CA) performs essential roles both early and late in the life cycle of HIV. Capsid is initially translated as the central region of the 55-kD Gag polyprotein, where it functions in viral assembly (*1*, *2*) and in packaging the cellular protein cyclophilin A (*3*). As the virus buds, Gag is processed by the viral protease to produce three discrete new proteins—matrix, capsid, and nucleocapsid—as well as several smaller peptides. After capsid has been liberated by proteolytic processing, it rearranges into the conical core structure that surrounds the viral genome at the center of the mature virus (*1*, *4*). Genetic analyses have revealed that capsid also performs essential roles as the virus enters,

Department of Biochemistry, University of Utah, Salt Lake City, UT 84132, USA.

*These authors contributed equally to this report.
†To whom correspondence should be addressed.